Chain Aggregation Process of Poly(methyl methacrylate) in the Mixed Solvent *tert*-Butyl Alcohol + Water

Yoshiki Nakamura, Naoki Sasaki, and Mitsuo Nakata*

Department of Polymer Science, Faculty of Science, Hokkaido University, Kita-ku, Sapporo 060-0810, Japan

Received July 13, 2001; Revised Manuscript Received November 13, 2001

ABSTRACT: To study a chain aggregation process, dilute solutions of poly(methyl methacrylate) in the mixed solvent *tert*-butyl alcohol + water (2.5 vol %) with the molecular weight $m = 1.57 \times 10^6$ were quenched to below the phase-separation temperature and scattered intensities were measured. The light-scattering measurement was carried out in the concentration range from 1.5×10^{-4} to 5.6×10^{-4} g/cm^3 for a time period of several hours. By using the Guinier plot, the weight-average molecular weight $\langle M\rangle_w$ and *z*-average square radius $\langle R^2\rangle_z$ of clusters of polymer chains were determined as a function of time t (min) and concentration c (g/cm^3). The chain aggregation process exhibited an exponential growth of the reduced form $\langle M\rangle_w = M(0)\exp(gct)$ with $g = 34.8$ cm^3/(g min), where $M(0)$ is the value extrapolated to $t = 0$. A double-logarithmic plot of $\langle M\rangle_w$ vs $\langle R^2\rangle_z^{1/2}$ yielded a slightly curved line at small $\langle M\rangle_w$ and approached the relation $\langle M\rangle_w \sim \langle R^2\rangle_z^{3/2}$. These characteristics of the observed chain aggregation process were consistent with the Smoluchowski equation with the collision kernel $(i + j)$ for i-mer and j-mer, and the relation $R_k \sim (mk)^{1/3}$ between the radius R_k and the molecular weight mk for k-mer was deduced from an analysis of the experimental data based on the Smoluchowski equation. The chain aggregation process observed for a long time period was not explained by a diffusion-limited aggregation mechanism but was explained by a reaction-limited one.

I. Introduction

Phase-separation processes in dilute polymer solutions may be studied precisely by static light-scattering experiments. Since the molecular weight and size of a single polymer chain are large enough to be determined by light scattering, the phase-separation process could be measured from the very initial stage at which clusters of a few polymer chains start to be formed. However, the chain aggregation process can be characterized by the time evolution of the cluster size distribution and the cluster structure, while the light-scattering experiment gives the time evolution of the weight-average molecular weight $\langle M\rangle_w$ and the *z*-average mean-square radius $\langle R^2\rangle_z$ of clusters of polymer chains. Therefore, to reveal the cluster aggregation process, the experimental data of $\langle M\rangle_w$ and $\langle R^2\rangle_z$ should be analyzed by a relevant theoretical prediction.

Phase-separation process depends strongly on a specific nature of polymer segment and solvent as well as the polymer concentration and molecular weight. For example, the phase separation occurs rapidly for polystyrene in cyclohexane[1] and very slowly for poly(*N*-isopropylacrylamide) in water.[2] We found that dilute solutions of poly(methyl methacrylate) (PMMA) underwent very slow phase separation, which allowed us to study the phase-separation process and also the chain collapse process by static light-scattering experiments.[3−7] The slow chain collapse is a parallel phenomenon to the slow phase separation because of a common aggregation mechanism specific to the nature of polymer segment and solvent.

In the previous studies,[4,5] we observed phase-separation processes for the dilute solutions of PMMA in isoamyl acetate with the molecular weight $m \times 10^{-6} =$ 2.35 and 4.4 at 25.0 and 30.0 °C, respectively. The processes were measured for a time period of several hours or more after quench of the solutions and, $\langle M\rangle_w$ and $\langle R^2\rangle_z$ of clusters of polymer chains were determined as a function of the time t and concentration c. Each plot of $\ln\{\langle M\rangle_w/M(0)\}$ and $\ln\{\langle R^2\rangle_z/R^2(0)\}$ vs ct was represented by a straight line for both the processes, where $M(0)$ and $R^2(0)$ were the values extrapolated to $t = 0$. The experimental relation between $\langle M\rangle_w$ and $\langle R^2\rangle_z$ was represented by $\langle R^2\rangle_z \sim \langle M\rangle_w^{2/D_p}$ with $D_p = 2.86 \pm 0.03$ for $m = 2.35 \times 10^6$ and 3.06 ± 0.02 for $m = 4.4 \times 10^6$. The slow exponential growth of the clusters cannot be attributed to a diffusion-limited cluster aggregation (DLCA) but to a reaction-limited cluster aggregation (RLCA).[8] The behavior of $\langle M\rangle_w$ was in agreement with the Smoluchowski equation with the collision kernel $i + j$ for i-mer and j-mer.[9,10] Thus, the equation was used to analyze the behavior of $\langle R^2\rangle_z$ and observed scattering function. The obtained relation between $\langle M\rangle_w$ and $\langle R^2\rangle_z$ was explained in terms of the cluster size distribution and the size dependence of the cluster structure. With increasing cluster size, the polymer segment density increased rapidly for small size clusters and approached a constant value for large clusters.

Recently,[6] we studied phase-separation processes for dilute solutions of PMMA in the mixed solvent *tert*-butyl alcohol + water at 2.5 vol % of water to reveal the effect of solvent nature on the chain aggregation process. Both *tert*-butyl alcohol and water are nonsolvents for the polymer, but an addition of small amount of water to the alcohol makes the mixture a good solvent for the polymer.[11] Thus, the mixed solvent may be very different from the single solvent isoamyl acetate in interaction with PMMA. The Θ-temperature of the solution of PMMA in the mixed solvent has been determined to be 41.5 °C.[7] In the study of the aggregation in the mixed solvent, dilute solutions for the molecular weight $m =$ 1.57×10^6 were quenched to 25.0 and 30.0 °C below

10.1021/ma011225c CCC: $22.00
Published on Web 01/11/2002

the phase-separation temperature. In the first 30 min after the quench, the polymer chains collapsed to equilibrium globules and scattered intensities were measured for a time period from hours to days to determine $\langle M\rangle_w$ and $\langle R^2\rangle_z$. At each temperature, both the plots of $\ln\langle M\rangle_w$ and $\ln\langle R^2\rangle_z$ vs time t yielded curved lines. The initial slopes of the lines were proportional to the concentration c. Thus, the reduced relations of $\langle M\rangle_w/M(0) = \exp(gct)$ and $\langle R^2\rangle_z/R^2(0) = \exp(hct)$ were obtained only at small ct. The observed very slow growth of clusters demonstrated a reaction-limited cluster aggregation of polymer chains as in the case of PMMA in isoamyl acetate. However, since the curved lines of $\ln\langle M\rangle_w$ vs time t could not be compared with the Smoluchowski equation, the cluster size distribution and cluster structure could not be deduced from the observed average values of $\langle M\rangle_w$ and $\langle R^2\rangle_z$. A close inspection of the chain aggregation processes at 25.0 and at 30.0 °C suggested that the exponential growth of $\langle M\rangle_w$ and $\langle R^2\rangle_z$ could occur at slightly higher temperatures.

In this study, we measured the chain aggregation process of PMMA with $m = 1.57 \times 10^6$ in the mixed solvent *tert*-butyl alcohol + water(2.5 vol %) at 33.0 °C to reveal the cluster size distribution and cluster structure. The data of $\langle M\rangle_w$ and $\langle R^2\rangle_z$ obtained for clusters of polymer chains were represented as a function of ct, and $\langle M\rangle_w$ exhibited the exponential growth in the whole experimental time region. Thus, the Smoluchowski equation with the collision kernel $i + j$ was used to analyze the experimental data. As predicted from the Smoluchowski equation,[12,13] the asymptotic relation $\langle M\rangle_w \sim \langle R^2\rangle_z^{3/2}$ was obtained at large ct, where the cluster size distribution was very wide such as $\langle M\rangle_w/\langle M\rangle_n > 5$ with $\langle M\rangle_n$ being the number-average molecular weight of clusters. The chain aggregation process in the mixed solvent was essentially the same as that in isoamyl acetate irrespective of different nature of the solvents.

II. Experiment and Data Analysis

The PMMA sample M19-F6 used in the present study is the same as that in previous studies[6,7] and has the weight-average molecular weight $m_w = 1.57 \times 10^6$ and characteristic ratio $\langle s^2\rangle_z/m_w = 6.1 \times 10^{-4}$ nm^2 mol/g, which gives a measure for the molecular weight distribution as $m_w/m_n = 1.17$.[14] The *tert*-butyl alcohol was fractionally distilled immediately before use. The water was purified by a standard method.

The present study was performed with the mixed solvent *tert*-butyl alcohol(1) + water(2) at the volume fraction $u_2 = 0.025$. The mixed solvent behaves as a single solvent in light-scattering measurements because of the vanishing derivative dn_o/du_2 of the refractive index n_o near $u_2 = 0.025$.[15] The refractive index increment dn/dc(cm^3/g) for the polymer solution at $u_2 = 0.025$ was measured to be 0.1113 at 35.0 °C, 0.1169 at 50.0, and 0.1220 at 65.0. These values give the temperature t (°C) dependence of $dn/dc = 0.0986 + 3.6 \times 10^{-4}\, t$, which agrees with the previous relation within an error of 1% in the range from 20 to 55 °C.[15]

The static light-scattering measurements were carried out at angular intervals of 15° in the range from 30 to 150° with unpolarized incident light at 435.8 nm of a mercury arc. For the measurements, four solutions at the concentrations c (10^{-4} g/cm^3) = 1.482, 2.773, 4.134, and 5.560 at 33.0 °C were prepared in each optical cell of 18 mm i.d. and 1 mm wall thickness. The solutions were filtered twice through a Sartorius membrane filter (SM 116, 0.45 μm) for optical clarification and stored in the dark at the Θ-temperature under saturated vapor of the mixed solvent. The solutions were quenched to 33.0 °C from the Θ-temperature, and measurements of scattered intensities were started 30 min after the quench on account of the thermal equilibration. During the measurements the solutions were transparent by eye and the multiple scattering effect was negligibly small.

Light-scattering data obtained at an angle θ were analyzed in the form of the excess Rayleigh ratio R_θ estimated as the difference between scattered intensities from solution and solvent. For a dilute solution under the Θ-condition, R_θ can be related to the molecular weight m and the scattering function $P_c(q)$ for a single polymer chain by[16]

$$R_\theta/Kc = mP_c(q) \tag{1}$$

where K and the argument q are defined by $K = (2\pi^2 n_o^2/N_A\lambda^4)(dn/dc)^2$ and $q = (4\pi n/\lambda)\sin(\theta/2)$. Here, N_A is Avogadro's number, λ is the wavelength of incident light in a vacuum, and n is the refractive index of the solution. In eq 1, the polymer is assumed tacitly to be monodisperse. We will hereafter use m for the molecular weight of a polymer and M for the molecular weight of a cluster of polymers.

In an aggregation process of polymer chains, the concentration c of total polymer is constant and expressed as the sum $c = \sum_k c_k$, where c_k is the concentration of the k-mer and c_1 is that of monomer $k = 1$ (single polymer chain). The optical constant K is unchanged in the process; dn/dc becomes independent of the molecular weight for $m > 10^4$ and the molecular weight can be estimated correctly for PMMA in a coil state and in a globule state with the same value of dn/dc.[7] Accordingly, R_θ is given by the sum $\sum_k Kc_kM_kP_k(q)$ with the molecular weight M_k (=km) and scattering function $P_k(q)$ for k-mer, and is expressed as

$$R_\theta/Kc = \langle M\rangle_w\langle P(q)\rangle_z \tag{2}$$

with

$$\langle M\rangle_w = \sum_k M_kc_k/\sum_k c_k \tag{3}$$

and

$$\langle P(q)\rangle_z = \sum_k P_k(q)M_kc_k/\sum_k M_kc_k \tag{4}$$

Here, $\langle M\rangle_w$ and $\langle P(q)\rangle_z$ are the weight-average molecular weight and z-average scattering function for clusters. For spherical particles, eq 2 can be expressed by the approximate form[17]

$$\ln(R_\theta/Kc) = \ln\langle M\rangle_w - (1/5)\langle R^2\rangle_z q^2 \tag{5}$$

where $\langle R^2\rangle_z$ is the z-average square radius of clusters. To determine $\langle M\rangle_w$ and $\langle R^2\rangle_z$ of clusters, light-scattering data were analyzed by the Guinier plot based on eq 5.

III. Experimental Results

Figure 1 shows the time evolution of scattered intensities from the solution at $c = 4.134 \times 10^{-4}$ g/cm^3 by the Guinier plot due to eq 5. The plots from the bottom to the top were obtained at 30, 60, 90, 120, 150, 180, 210, 240, and 270 min after quench to 33.0 °C. The solid lines describe the behavior of data points. On the basis of eq 5, $\langle M\rangle_w$ (g/mol) and $\langle R^2\rangle_z$ (nm^2) at each time were estimated from the intercept and the initial slope of the line, respectively. Light-scattering data at other concentrations behaved similarly and were analyzed in the same way. Figures 2 and 3 show the semilogarithmic plots of $\langle M\rangle_w$ and $\langle R^2\rangle_z$ vs the time t (min) for solutions at c (10^{-4} g/cm^3) = 1.482 (○), 2.773 (△), 4.134 (□), and

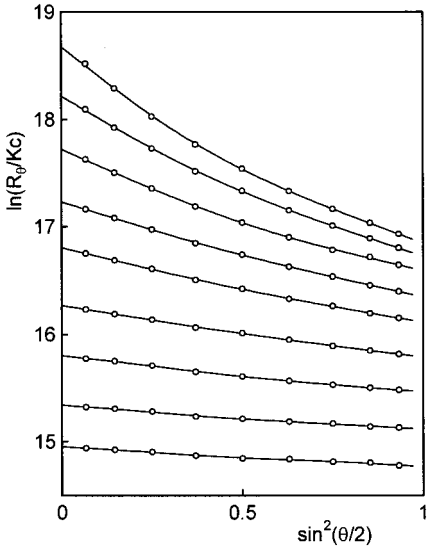

Figure 1. Time evolution of scattered intensities by the Guinier plot of $\ln(R_\theta/Kc)$ vs $\sin^2(\theta/2)$ at $c = 4.134 \times 10^{-4}$ g/cm^3 for PMMA in the mixed solvent *tert*-butyl alcohol + water (2.5 vol %) with $m = 1.57 \times 10^6$. Curves from the bottom were obtained 30, 60, 90, 120, 150, 180, 210, 240, and 270 min after quench to 33.0 °C.

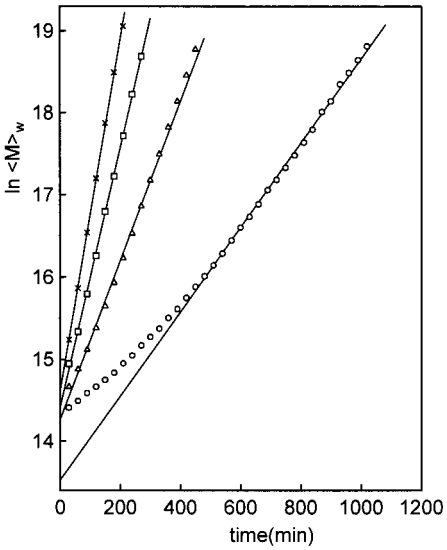

Figure 2. Semilogarithmic plot of weight-average molecular weight $\langle M\rangle_w$ (g/mol) of clusters vs time t (min) after quench to 33.0 °C. Data points were obtained at c (10^{-4}g/cm^3) = 1.482 (○), 2.773 (△), 4.134 (□), and 5.560 (×).

5.560 (×), respectively. These plots appear to be represented by straight lines with the relations

$$\ln \langle M\rangle_w = \ln M(0) + Gt \tag{6}$$

$$\ln \langle R^2\rangle_z = \ln R^2(0) + Ht \tag{7}$$

where $M(0)$ and $R^2(0)$ are the values extrapolated to $t = 0$. Table 1 gives the values of $M(0)$, $R^2(0)$, G, and H estimated from the straight lines in Figures 2 and 3. The data points at the lowest concentration $c = 1.482 \times 10^{-4}$ g/cm^3 deviate considerably from the straight line at small t. This trend is also observed slightly in the plots at $c = 2.773 \times 10^{-4}$ g/cm^3.

Figure 4 shows the plots of G and H against c. The data points fit to the straight line passing through the origin. This means that each of the reduced plots of ln-

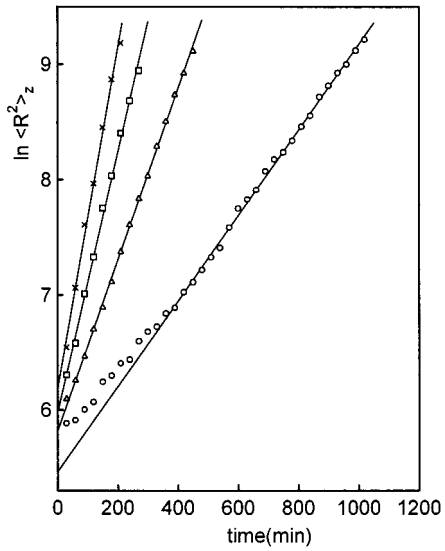

Figure 3. Semilogarithmic plot of z-average mean-square radius $\langle R^2\rangle_z$ (nm^2) of clusters vs time t (min) after quench to 33.0 °C. Symbols of data points are the same as in Figure 2.

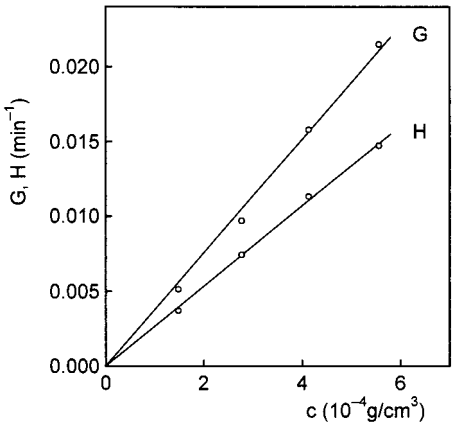

Figure 4. Slope G for the plot of $\ln\langle M\rangle_w$ vs t and slope H for $\ln \langle R^2\rangle_z$ vs t as a function of the concentration c for the chain aggregation processes at 33.0 °C.

Table 1. Concentration Dependence of the Parameters $M(0)$ and G in Eq 6, and $R^2(0)$ and H in Eq 7

c (10^{-4} g/cm^3)	$M(0)$ (10^6 g/mol)	G (10^{-3} min^{-1})	$R^2(0)$ (10^2 nm^2)	H (10^{-3} min^{-1})	$R(0)/M^{1/3}(0)$ (nm mol$^{1/3}$/g$^{1/3}$)
1.482	0.74	5.14	2.36	3.71	0.170
2.773	1.55	9.69	3.35	7.44	0.158
4.134	1.80	15.8	3.94	11.3	0.163
5.560	2.19	21.5	4.87	14.7	0.170

$\{\langle M\rangle_w/M(0)\}$ and $\ln\{\langle R^2\rangle_z/R^2(0)\}$ vs ct should give a straight line. Figure 5 shows the reduced plots for $\langle M\rangle_w$ and $\langle R^2\rangle_z$ by open circles and triangles, respectively. As indicated by Figure 4, data points at different concentrations are fitted to the straight lines. The data points deviated from the straight lines in Figures 2 and 3 are omitted. Thus, the observed chain aggregation process seems to be expressed by the relations

$$\langle M\rangle_w/M(0) = \exp(gct), \tag{8}$$

$$\langle R^2\rangle_z/R^2(0) = \exp(hct), \tag{9}$$

where the coefficients g and h were estimated as $g = 34.8$ cm^3/(g min) and $h = 25.0$ cm^3/(g min) from the straight lines in Figure 5.

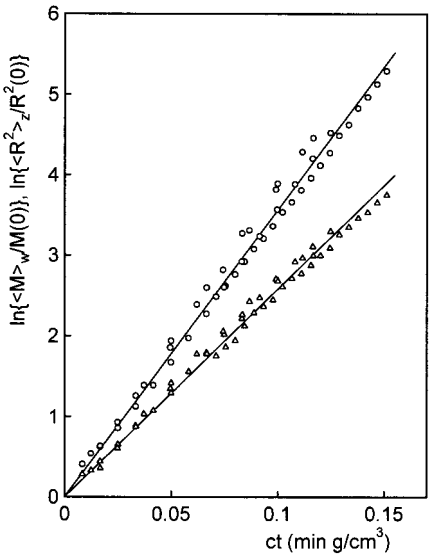

Figure 5. Reduced plots of $\ln\{\langle M\rangle_w/M(0)\}$ (circles) and $\ln\{\langle R^2\rangle_z/R^2(0)\}$ (triangles) vs ct at various concentrations and times after quench to 33.0 °C. From the plots the coefficients in eqs 8 and 9 were estimated to be $g = 34.8$ cm^3/(g min) and $h = 25.0$ cm^3/(g min).

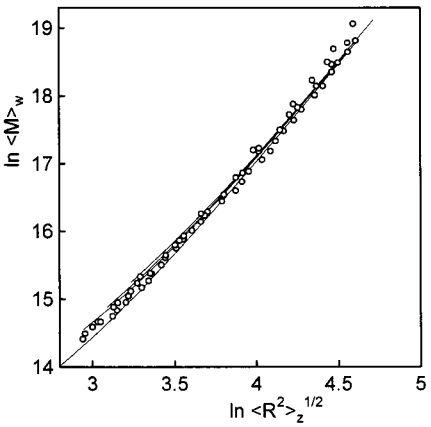

Figure 6. Double-logarithmic plot of $\langle M\rangle_w$ vs $\langle R^2\rangle_z^{1/2}$ for data at various concentrations and times after quench to 33.0 °C. The four thin lines are calculated with eqs 14, 16 with $A = 0.140$ and 18 with B/m ($=g/2$) $= 17.4$ cm^3/(g min) at the experimental concentrations.

Figure 6 shows the plot of $\ln\langle M\rangle_w$ vs $\ln\langle R^2\rangle_z^{1/2}$ for the data at the four concentrations. The points deviated from the straight lines in Figures 2 and 3 are also plotted indistinguishably. The data points at the different concentrations construct a slightly curved composite line. The curvature is clearly observed by seeing the plot in the direction of an array of the points. Equations 8 and 9 predict a composite but straight line for the plot. This discrepancy will be discussed with the conclusion that eq 9 is an approximate expression for $\langle R^2\rangle_z$ on the basis of the Smoluchowski equation. In Figure 6, the plot at large $\langle R^2\rangle_z$ appears to be expressed by the power law

$$\langle R^2\rangle_z^{1/2} = A_p\langle M\rangle_w^{1/D_p} \tag{10}$$

with $D_p = 3$.

Figure 7 shows the plot of $\langle P(q)\rangle_z$ ($=R_\theta/Kc\langle M\rangle_w$) vs $\langle R^2\rangle_z q^2$ for data obtained at different concentrations and times (c, 10^{-4}g/cm^3; t, min) as ○ (1.482, 1020), △ (2.773, 450), □ (4.134, 270), and × (5.560, 210). The data points

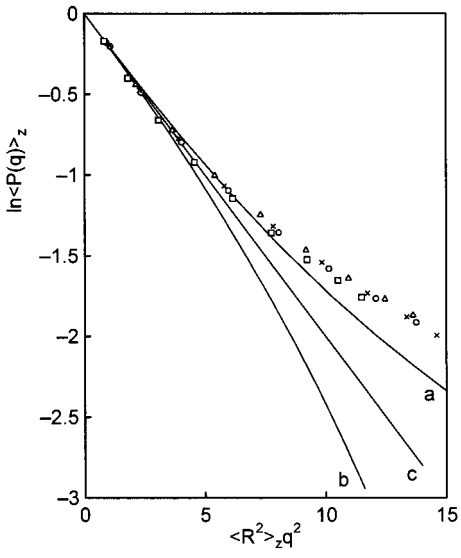

Figure 7. Guinier plot of the scattering function $\langle P(q)\rangle_z$ against $\langle R^2\rangle_z q^2$. Data points were obtained at different concentrations and times (c, 10^{-4}g/cm^3; t, min) as ○ (1.482, 1020), △ (2.773, 450), □ (4.134, 270), and × (5.560, 210). Line a was calculated at the same values of c and t as the data points by using eqs 4, 15, 18, and 21. Line b is for monodisperse spheres. The straight line c has an initial slope of $^1/_5$ for spheres.

appear to fall on a single composite line in the whole experimental range of $\langle R^2\rangle_z q^2$.

We carried out measurements of the dissociation of polymer clusters of large size. For this purpose a sudden temperature rise from 33.0 to 41.5 °C was given to the solutions at c (10^{-4}g/cm^3) = 1.482, 2.773, 4.134, and 5.560, when the measurements of the cluster aggregation process for the time periods of 1020, 450, 270, and 210 min had been completed, respectively. At these last stages the average size of the clusters reached $\langle M\rangle_w \sim 1.5 \times 10^8$ g/mol and $\langle R^2\rangle_z^{1/2} \sim 100$ nm. At 30 min after the temperature rise, scattered intensities were measured and analyzed by the usual Zimm plot as shown in Figure 8. From the plot we obtained $m = 1.50 \times 10^6$ and the characteristic ratio $\langle s^2\rangle/m = 5.8 \times 10^{-4}$ nm^2 mol/g, which demonstrated that the clusters dissociated thoroughly within 30 min after the temperature rise.

IV. Analysis with the Smoluchowski Equation

Smoluchowski formulated aggregation kinetics in terms of cluster−cluster collisions.[9] The k-mer can be formed by a collision of i-mer and j-mer ($k = i + j$) and converted into a larger size cluster by collisions with other clusters. By assuming a random distribution of clusters in a solution, the time evolution of the number $N_k(t)$ of k-mer ($k = 1, 2, ...$) in unit volume was derived with the collision kernel K_{ij} in the form

$$dN_k/dt = (1/2)\sum_{i+j=k} K_{ij}N_iN_j - N_k\sum_j K_{kj}N_j. \tag{11}$$

Equation 11 has been solved only for $K_{ij} = 1$, $i + j$, ij, and their linear combinations, while the moments of the distribution defined by $Q_n(t) = \sum_k k^n N_k(t)$ can be easily calculated by[18,19]

$$dQ_n/dt = (1/2)\sum_i\sum_j[(i+j)^n - i^n - j^n]\,K_{ij}N_iN_j \tag{12}$$

The first moment Q_1 represents the total number N of monomers and should be constant. The number-average

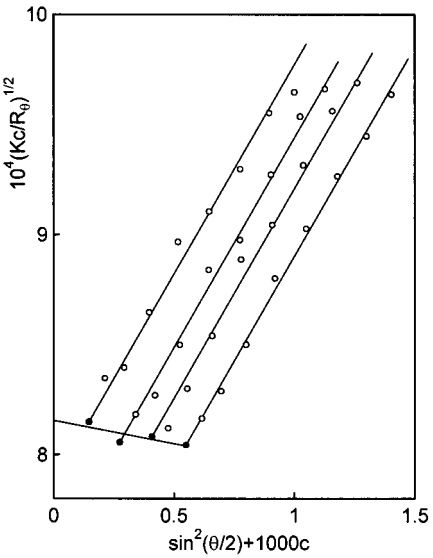

Figure 8. Chain dissociation experiment by sudden temperature rise. The Zimm plot was constructed by scattered intensities from the solutions which were given by a sudden temperature rise from 33.0 to 41.5 °C after a completion of the measurement of chain aggregation process. The scattered intensities were determined 30 min after the temperature rise.

molecular weight and weight-average molecular weight of clusters are expressed as $\langle M\rangle_n = mQ_1/Q_0$ and $\langle M\rangle_w = mQ_2/Q_1$, respectively. For a given form of K_{ij}, an explicit expression of $Q_n(t)$ can be obtained for an initial condition. In the present experiment, the initial condition is given by $N_1(0) = N\ (=c/m)$ and $N_i(0) = 0\ (i \geq 2)$. Thus, for $K_{ij} = B(i + j)$ with B as a constant, eq 12 gives

$$\langle M\rangle_n = m\ \exp(Bct/m) \tag{13}$$

$$\langle M\rangle_w = m\ \exp(2Bct/m). \tag{14}$$

Both eqs 8 and 14 exhibit exponential growth of clusters with the reduced time ct. In eq 8, $M(0)$ depends on c due to interaction between polymer chains and gives an apparent molecular weight, while the factor g is independent of c and holds the relation $2B/m = g = 34.8$ cm^3/(g min).

We assume that the relation between the molecular weight $M_k\ (=km)$ and the radius R_k for k-mer could be expressed by

$$R_k = A(km)^{1/D} \tag{15}$$

The exponent D in eq 15 is dominated by the structure of cluster, while D_p in eq 10 is dominated by the cluster size distribution as well as the cluster structure and is not constant. By using eq 15, the z-average square radius of clusters is written as

$$\langle R^2\rangle_z = A^2\langle M^{2/D}\rangle_z \tag{16}$$

with

$$\langle M^{2/D}\rangle_z = \sum_k (km)^{2/D}k^2N_k/\sum_k k^2N_k \tag{17}$$

It is possible to calculate $\langle M^{2/D}\rangle_z$ with the Smoluchowski equation provided that the distribution $N_k(t)$ is given explicitly.

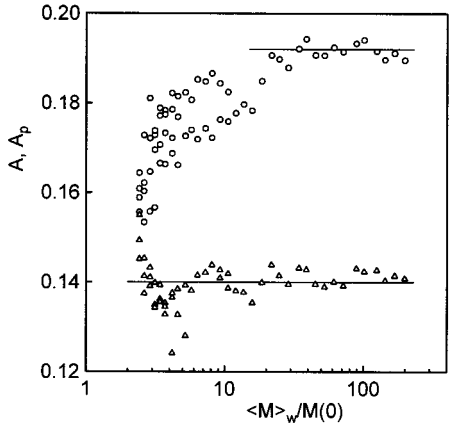

Figure 9. Experimental values of A_p (circles) in eq 10 with $D_p = 3$ and calculated values of A in eq 15 with $D = 3$ (triangles) as a function of $\langle M\rangle_w/M(0)$.

For the present initial condition, the solution of eq 11 with $K_{ij} = B(i + j)$ has been written explicitly as[18,19]

$$N_k(t) = N(1 - b)e^{-kb}(kb)^{k-1}/k! \tag{18}$$

with

$$b = 1 - e^{-(B/m)ct}$$

It should be noted that $N_k(t)$ depends on time t through b with the reduced time ct. We assumed $D = 3$ in eq 15, because polymer chains for $m = 1.57 \times 10^6$ were found in the globule state at 33.0 °C.[7] Since the value of m $(=M(0))$ at each concentration has been estimated as shown in Table 1 and the constant B is given by $B = mg/2$, we can calculate $\langle M^{2/D}\rangle_z$ as a function of time at each concentration. Then, coefficient A in eq 16 can be estimated as the ratio of the observed value of $\langle R^2\rangle_z$ to the calculated value of $\langle M^{2/D}\rangle_z$. In this calculation we omitted the data of $\langle R^2\rangle_z$ which deviate from the straight line at small t in Figure 3. In Figure 9 the calculated A(triangles) is plotted against $\ln\{\langle M\rangle_w/M(0)\}$ together with A_p (circles) obtained from experimental data by eq 10 with the fixed value $D_p = 3$. Coefficient A exhibits a constant value near 0.140 independent of the concentration in the region of $\langle M\rangle_w/M(0) > 6$. The behavior of data points at small $\langle M\rangle_w/M(0)$ is not clear because of an experimental uncertainty due to the small initial slope of the Guinier plot at small t as shown in Figure 1. On the other hand, A_p increases with increasing $\langle M\rangle_w/M(0)$ and has a constant value near 0.192 at large $\langle M\rangle_w/M(0)$. The value of A obtained at the lowest concentration seems to be artificial because of the small values of $M(0)$ and $R^2(0)$ and should be taken with reservation. However, it should be noticed that the constant values of A independent of the concentration stem from the constant value of $R(0)/M^{1/3}(0)(=A(0))$ given in Table 1.

Using eqs 14 and 16 with $A = 0.140$, we calculated $\langle M\rangle_w$ and $\langle R^2\rangle_z$ as a function of time at each experimental concentration to reproduce the plot of $\ln\langle M\rangle_w$ against $\ln\langle R^2\rangle_z$. In Figure 6, the thin lines are given by the calculation. These lines have curvatures and depend on the concentration slightly at small $\ln\langle M\rangle_w$, while the lines appear to converge on a single straight line with $D_p = 3$ at large $\ln\langle M\rangle_w$. This behavior of the calculated lines is in accord with that of the data point. It is interesting to evaluate an asymptotic value of the coefficient A_p in eq 10 with $D_p = 3$ at large $\ln\langle M\rangle_w$.

Equation 18 has been shown to have an approximate expression for $ct \gg (m/2B)\ln(k/2)$ as[12,13]

$$N_k(t) \cong N\{(1-b)/(2\pi)^{1/2}bk^{3/2}\}\exp\{-(1-b)^2k/2\} \quad (19)$$

Using eqs 16 with $D = 3$ and 19, we have

$$\langle R^2\rangle_z \cong 1.94A^2\langle M\rangle_w^{2/3} \quad (20)$$

at large ct. This relation gives $D_p = 3$ and is in agreement with eq 10 obtained at large ct. Moreover, the relation $A_p = 1.94^{1/2}A$ yields $A_p = 0.195$ which agrees with the experimental value 0.192. In the asymptotic range at large ct the polydispersity of cluster size becomes large. The width of the cluster size distribution can be expressed by the ratio $\langle M\rangle_w/\langle M\rangle_n$ according to the methodology of the polymer characterization and is given by $\langle M\rangle_w/\langle M\rangle_n = \exp(Bct/m)$. In Figure 9, the constant value of A_p is obtained in the range $\langle M\rangle_w/\langle M\rangle_n > 5$. Thus, the power law of eq 20 characterizes the aggregation process in the region of large polydispersity.

Coefficient A in eq 15 with $D = 3$ gives a measure for packing of polymer chains in a cluster, because $A^3 = R_k^3/M_k$ is proportional to the specific volume of a cluster. The radius R of a single polymer chain has been estimated as $R = 21$ nm from the observed mean-square radius $\langle s^2\rangle = 260$ nm^2 with the relation $R = \{(5/3)\langle s^2\rangle\}^{1/2}$, because the polymer chain at 33.0 °C has been found in a globule state. Thus, we obtain $R^3/m = 0.0059$ nm^3 mol/g for a single polymer chain, while we have $A^3 = 0.0027$ nm^{3}mol/g for a cluster. A^3 is roughly a half of R^3/m, which implies that the polymer-segment density in a cluster is twice as high as that in a single polymer chain. The segment mass concentration $c_s = 1/\{(4\pi/3)N_AA^3\}$ in a cluster can be estimated to be 0.067 g/cm^3 for a single polymer and 0.144 g/cm^3 for a cluster. The constant value of A^3 independent of the average cluster size and the concentration suggests that the concentration $c_s = 0.144$ g/cm^3 might be compared with that of the concentrated phase in macroscopic two-phase equilibrium. It would be intriguing to measure the two-phase coexistence curve for the present system.

The scattering function $\langle P(q)\rangle_z$ at each concentration and each time can be calculated by using eqs 4 and 18 as in the case of $\langle M^{2/D}\rangle_z$. Assuming spherical clusters, the scattering function $P_k(q)$ for k-mer is to be expressed by[17]

$$P_k(q) = \{[3/(R_kq)^3][\sin(R_kq) - (R_kq)\cos(R_kq)]\}^2 \quad (21)$$

where R_k is given by eq 15 with $D = 3$ and $A = 0.140$. We calculated $\langle P(q)\rangle_z$ at the same values of c and t as those for the scattering data in Figure 7. The four calculated scattering functions agreed closely with each other and yielded the single curve a in Figure 7. The observed scattering functions also give a composite line independent of the concentration. The line b is calculated for monodisperse spheres, and the straight line c is given with the initial slope of $^1/_5$ for spheres. The line a is very close to the data points, when compared with lines b and c. The rapidly increasing difference between lines a and b with increasing $\langle R^2\rangle_zq^2$ is caused by the polydispersity of cluster size. According to the relation $\langle M\rangle_w/\langle M\rangle_n = \exp(Bct/m)$, the scattering functions in Figure 7 have been obtained at the different polydispersity as $\langle M\rangle_w/\langle M\rangle_n = 13.7$ (○), 8.8 (△), 8.4 (□), and 9.6 (×). These values are extremely large when compared with the molecular weight distribution $\langle M\rangle_w/\langle M\rangle_n = 2$ typical for synthetic polymers prepared by usual method.

V. Discussion and Conclusion

In a previous study,[6] the chain aggregation process was studied for the same system as the present one at the different temperatures as 25.0 and 30.0 °C. The time evolution of the average size of clusters was discussed in terms of $\langle M\rangle_w$ and $\langle R^2\rangle_z$. Each double-logarithmic plot of $\langle M\rangle_w$ vs $\langle R^2\rangle_z$ at 25.0 and 30.0 °C was represented by a single straight line. The plots of ln $\langle M\rangle_w$ and ln$\langle R^2\rangle_z$ vs ct were considerably curved and constructed composite curves only in the region of small ct at each temperature. The initial slope g for ln $\langle M\rangle_w$ vs ct was determined unambiguously to be $g = 5.0$ at 25.0 °C and 16.9 at 30.0 °C, which are smaller than the present value $g = 34.8$ at 33.0 °C. Furthermore, we determined the phase-separation temperature T_p of the dilute solutions to be 35.7, 36.2, 36.6, and 36.7 °C at c (10^{-4} g/cm^3) = 1.43, 2.73, 4.17, and 5.58, respectively.[6] Since these concentrations are very close to the present ones, the observed phase-separation temperature can be applied to the present study. The strong temperature dependence of g indicates that a slight decrease of temperature gives rise to a large decrease of the rate of the chain aggregation. This implies that the chain aggregation processes at a constant temperature distance from the phase-separation temperatures could not be expressed by the composite line as given in Figure 5. That is, the rate of the aggregation is not specified by the temperature distance from a phase-separation temperature but by the absolute temperature. In the previous study, we also estimated the second virial coefficient A_2 as a function of temperature from the light-scattering data. The observed values of A_2 exhibited a clear minimum near 33.0 °C and increased with decreasing temperature in the limited range from 33 to 25 °C. According to our intuition for the phase-separation process, this behavior of A_2 is compatible with the temperature dependence of the observed chain aggregation rate: The chain aggregation is to become faster with decreasing A_2. However, this is not the case for the chain aggregation processes just below the phase-separation temperature and near 20.0 °C where the rapid phase-separation has been suggested.[7]

The aggregation process at 33.0 °C can be compared with the Smoluchowski equation for cluster−cluster aggregation with the collision kernel $(i + j)$ for i-mer and j-mer because of the reduced linear plot of ln$\langle M\rangle_w$ vs ct in Figure 5. The observed aggregation process was analyzed consistently by the equation assuming $D = 3$ in eq 15 on the basis of eq 18. The coefficient A was determined to be a constant independent of time and concentration, which may indicate a constant polymer segment density in clusters. The relation between $\langle M\rangle_w$ and $\langle R^2\rangle_z$ obtained at large ct was represented by eq 10 with $D_p = 3$ and $A_p = 0.192$, which was deduced analytically from the asymptotic expression of eq 19. As shown in Figure 7, the calculated scattering function given by the curve a cannot describe the experimental data points at large $\langle R^2\rangle_zq^2$ satisfactorily. This behavior may reflect a cluster structure slightly different from a sphere with a uniform segment density rather than a deviation from the cluster size distribution of eq 18. Because of the constant value of A, the polydispersity of the cluster size is directly reflected to the curved line in Figure 6. In light of Figure 9 the asymptotic behavior

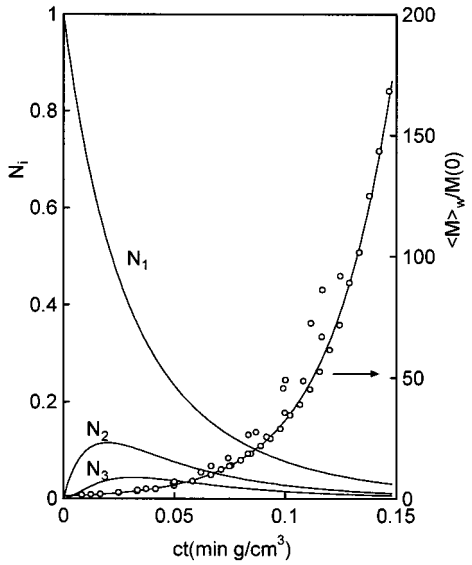

Figure 10. Cluster size distribution as a function of ct. N_1, N_2, and N_3 calculated by eq 18 with $2B/m = 34.8$ cm^3/(g min) and normalized by $\sum_k kN_k = 1$. Data points represent the weight-average number $\langle M\rangle_w/M(0)$ of chains in a cluster.

with $D_p = 3$ is seen in the region where the polydispersity exceeds $\langle M\rangle_w/\langle M\rangle_n \sim 5$. It is remarkable that the time-evolving system with extremely wide cluster size distribution is expressed by a simple relation of eq 20. It should be noticed that the exponent D_p depends on the averaging method for M and R, i.e., experimental method for determining M and R. For example the use of the number-average molecular weight $\langle M\rangle_n$ instead of $\langle M\rangle_w$ would yield $D_p = 1.5$.

It is interesting to visualize a time evolution of the cluster size distribution given by eq 18. Figure 10 shows N_1, N_2, N_3, and $\langle M\rangle_w/M(0)$ as a function of ct, where N_i is normalized as $\sum_k kN_k = 1$. The open circles represent experimental data for $\langle M\rangle_w/M(0)$. N_1 decreases monotonically with increasing ct because of the unidirectional cluster formation without dissociation. Each of N_2 and N_3 has a peak due to a balance of the cluster formation and conversion to larger size clusters. According to an analysis of eq 18, this is also the case for N_i ($i > 4$). The peak has a lower value and shifts to a larger ct with increasing k. The weight-average number $\langle M\rangle_w/M(0)$ of chains in a cluster starts from unity at $ct = 0$ and increases monotonically. It is obvious that the cluster size distribution becomes very broad at large ct.

Aggregations of colloidal particles have been studied in two different regimes: the fast aggregation process due to diffusion-limited cluster aggregation (DLCA) and the slow aggregation process due to reaction-limited cluster aggregation (RLCA).[8] The two aggregation processes have been distinguished by the rate of aggregation and the functional form of the time evolution of the cluster size distribution.[12,18] DLCA is represented by eq 11 with the collision kernel $K_{ij} = 8\pi D_t R$, where D_t and R are the diffusion constant and radius of a monomer, respectively.[10] For the present initial condition with monomers alone, eq 12 gives $\langle M\rangle_n = m(1 + 4\pi D_t RNt)$ and

$$\langle M\rangle_w = m(1 + 8\pi D_t RNt), \qquad (22)$$

where $1/(8\pi D_t RN)$ is a characteristic time and expressed as $3\eta/4kTN$ with the Stokes−Einstein relation $D_t = kT/(6\pi\eta R)$. Here, η is the viscosity coefficient and is roughly 10^{-3} Pa·s for the present mixed solvent. Thus, in the experimental range of the concentration, the characteristic time is estimated to be 10^{-2} s, which is smaller by several orders than the time period of the present aggregation process. The functional form of eq 22 for DLCA is different from that of eq 14, which has been known to characterize RLCA.[8] It is clear that the present aggregation process is controlled by the reaction-limited cluster aggregation.

In general, RLCA has been observed far from the equilibrium state. On the other hand, the present chain aggregation process is measured at a few degrees below the phase-separation temperature and is sensitive to the temperature change. The reaction between polymer clusters may be due to the reaction between polymer segments. Thus, the collapse of a single polymer chain is also expected to occur very slowly, because the reaction between segments belonging to different chains cannot be distinguished from the reaction of those belonging to a same chain. In fact, for the molecular weight $m \times 10^{-6} = 4.0$ and 12.2, we have observed a chain collapse process for a long time period from a few hours to a few weeks.[7] An inquiry for the origin of RLCA is out of the scope of this study. However, we suppose that the chain aggregation rate might depend on the content of water in the mixed solvent. An experiment with the mixed solvent of a different water content is under investigation.

In previous studies,[4,5] the chain aggregation process of PMMA in isoamyl acetate was measured for $m = 2.35 \times 10^6$ at 25.0 °C and for 4.4×10^6 30.0 °C by static light scattering. Since the observed chain aggregation processes were characterized by the exponential growth of eqs 8 and 9, the processes were analyzed by the Smoluchowski equation as in the present study. For the processes in isoamyl acetate, the obtained values of A in eq 15 showed a rapid decrease at small cluster size k and approached constant values with increasing k. The decrease of A at small k was more remarkable for $m = 4.4 \times 10^6$ than for $m = 2.35 \times 10^6$. This behavior disclosed a variation of the cluster structure with the cluster size k: the coalescence of polymer chains of large molecular weight may be difficult on account of a topological repulsion between polymer globules,[20] and the shape of a cluster of a few polymer chains may be different from a sphere. For the present solution of the low molecular weight $m = 1.57 \times 10^6$, the dependence of A on k is not expected from Figure 9. Thus, the polymer chains of low molecular weight may coalesce easily into a spherical cluster of a constant segment density independent of k.

References and Notes

(1) Chu, B.; Ying, Q.; Grosberg, A. Y. *Macromolecules* **1995**, *28*, 180.
(2) Wang, X.; Qiu, X.; Wu, C. *Macromolecules* **1998**, *31*, 2972.
(3) Nakata, M.; Nakagawa, T. *J. Chem. Phys.* **1999**, *110*, 2703.
(4) Nakata, M.; Nakagawa, T.; Nakamura, Y.; Wakatsuki, S. *J. Chem. Phys.* **1999**, *110*, 2711.
(5) Nakagawa, T.; Nakamura, Y.; Sasaki, N.; Nakata, M. *Phys. Rev. E* **2001**, *63*, 031803.
(6) Nakamura, Y.; Nakagawa, T.; Sasaki, N.; Yamagishi, A.; Nakata, M. *Macromolecules* **2001**, *34*, 5984.
(7) Nakamura, Y.; Sasaki, N.; Nakata, M. *Macromolecules* **2001**, *34*, 5992.
(8) Vicsek, T. In *Fractal Growth Phenomena*; Word Scientific: Singapore, 1989.
(9) Smoluchowski, M. V. *Z. Phys. Chem.* (*Munich*) **1917**, *92*, 129; *Phys. Z.* **1916**, *17*, 585.

(10) Chandrasekhar, S. *Rev. Mod. Phys.* **1943**, *15*, 1.
(11) Cowie, J. M. G.; Mohsin, M. A.; McEwen, I. *J. Polym.* **1987**, *28*, 1569.
(12) Lin, M. Y.; Klein, R.; Lindsay, H. M.; Weitz, D. A.; Ball, R. C.; Meakin, P. *J. Colloid Interface Sci.* **1990**, *137*, 263.
(13) von Schulthess, G. K.; Benedek, G. B.; De Blois, R. W. *Macromolecules* **1980**, *13*, 939.
(14) Nakata, M.; Kawate, K.; Ishitaka, Y. *Macromolecules* **1994**, *27*, 1825.
(15) Nakata, M. *Phys. Rev. E* **1995**, *51*, 5770.
(16) Kratochvil, P. In *Classical Light Scattering from Polymer Solution*; Elsevier: Amsterdam, 1987.
(17) Turkevich, J.; Hubbell, H. H. *J. Am. Chem. Soc.* **1951**, *73*, 1.
(18) Ziff, R. M. In *Kinetics of Aggregation and Gelation*; Family, F., Landau, D. P., Eds.; North-Holland: Amsterdam, 1984.
(19) Cohen, R. J.; Benedek, G. B. *J. Phys. Chem.* **1982**, *86*, 3696.
(20) Chuang, J.; Grosberg, A. Yu.; Tanaka, T. *J. Chem. Phys.* **2000**, *112*, 6434.

MA011225C